

# Porous Cobalt Oxide@Layered Double Hydroxide Core-Shell Architectures on Nickel Foam as Electrode for Supercapacitor

Zhang Luojiang<sup>1\*</sup>, Hui Kwan San<sup>2</sup>

1. Department of Electrical Engineering, The Hong Kong Polytechnic University, Hung Hom, Kowloon, Hong Kong, P. R. China; 2. School of Mathematics, University of East Anglia, Norwich, NR4 7TJ, United Kingdom

(Received 24 May 2018; revised 5 July 2018; accepted 9 July 2018)

**Abstract:** The high performance of an electrode relies largely on a scrupulous design of nanoarchitectures and smart hybridization of electroactive materials. A porous core-shell architecture in which one-dimensional cobalt oxide ( $\text{Co}_3\text{O}_4$ ) nanowire cores are grown on nickel foam prior to the growth of layered double hydroxide (LDH) shells is fabricated. Hydrothermal precipitation and thermal treatment result in homogeneous forests of 70-nm diameter  $\text{Co}_3\text{O}_4$  nanowire, which are wrapped in LDH-nanosheet-built porous covers through a liquid phase deposition method. Due to the unique core-shell architecture and the synergetic effects of  $\text{Co}_3\text{O}_4$  and NiAl-LDH, the obtained  $\text{Co}_3\text{O}_4$ @LDH electrode exhibits a capacitance of 1 133.3 F/g at a current density of 2 A/g and 688.8 F/g at 20 A/g (5.3 F/cm<sup>2</sup> at 9.4 mA/cm<sup>2</sup> and 3.2 F/cm<sup>2</sup> at 94 mA/cm<sup>2</sup>), which are better than those of the individual  $\text{Co}_3\text{O}_4$  nanowire. Moreover, the electrode shows excellent cycling performance with a retention rate of 90.4% after 3 000 cycles at a current density of 20 A/g.

**Key words:** core-shell; cobalt oxide; layered double hydroxide(LDH); nickel foam; supercapacitor(SC)

**CLC number:** O646

**Document code:** A

**Article ID:** 1005-1120(2018)04-0603-08

## 0 Introduction

As a bridge between capacitors and batteries, supercapacitors (SCs), also known as electrochemical capacitors, hold substantial promise for next-generation power devices due to their rapid charge and discharge rate, high power density, long lifespan, high reliability, and low maintenance cost<sup>[1-4]</sup>. To date, much efforts have been devoted to pseudocapacitor ( $\text{RuO}_2$ <sup>[5]</sup>,  $\text{MnO}_2$ <sup>[6]</sup> and conducting polymers<sup>[7]</sup> because they can achieve much higher charge storage than electrochemical double-layer capacitors (carbon materials<sup>[8-9]</sup>).

Among the pseudocapacitor materials, layered double hydroxide (LDH), which is composed of brucite-like host layers and charge-compensating interlayer anions, has attracted a great deal of attention because of their high redox activ-

ity, relatively low cost, and environmentally friendly features<sup>[10-11]</sup>. Besides the electrical double-layer capacitance acquired by their abundant slabs, in particular, several faradaic reactions of electrochemical active sites could occur on the surface or near the surface range for charge storage, leading to high energy storage and simultaneously maintaining a powerful performance<sup>[12]</sup>. It is thus currently the subject of intensive research to fabricate LDH with different morphologies and examine associated electrochemical properties. However, the key issues limiting the widespread applications rest with its low high-rate performance and poor cycle life, which are mainly caused by the intrinsic insulation and the highly packed morphology<sup>[13]</sup>. Therefore, it is crucial to enhance charge transfer kinetics and design rational architecture to fully utilize the redox reac-

\* Corresponding author, E-mail address: luojiang0901@163.com.

tions for high performance SCs. An effective way is to fabricate 1-D electroactive materials on conductive current-collecting substrates to form a binder-free electrode, which can provide fast ion and electron transfer as well as sufficient effective area between electrolyte ions and active materials for faradaic reactions. Practically, 3-D nickel foam (NF) has been applied to the substrate due to the relatively high surface area, conductivity and corrosion resistance to alkaline electrolyte<sup>[14]</sup>. Zhang et al. synthesized 1-D mesoporous  $\text{Co}_3\text{O}_4$  nanowire arrays on NF via a facial two-step strategy which showed a specific capacity of 1 160 F/g at 2 A/g and 820 F/g at 20 A/g<sup>[15]</sup>.

Currently, the hetero-structured 1-D nanowire architecture have attracted considerable attention in the energy storage due to the ingenious combination of an efficient exposure of active sites and synergetic effect between core and shell. For instance, the Co-oxide based cores are of great interests, because they do not just serve as an agent to increase the surface area but also contribute to the total capacitance owing to their own high electrochemical activities<sup>[16, 17]</sup>. Therefore, we reported a stepwise approach to design and fabricate 3-D porous  $\text{Co}_3\text{O}_4$ @LDH core-shell nanoarrays directly grown on NF as a binder-free electrode for supercapacitor(SC), where the 1-D  $\text{Co}_3\text{O}_4$  nanowires act as the “core” via a hydrothermal precipitation and thermal treatment and NiAl LDH nanosheets work as the “shell” layer through liquid phase deposition method. Such unique architecture can offer a large interfacial area for reaction, numerous channels for rapid diffusion of electrolyte ions, and fast electron transport, which endows the designed  $\text{Co}_3\text{O}_4$ @LDH electrode with an excellent capacitive performance. The as-prepared  $\text{Co}_3\text{O}_4$ @LDH hybrid electrode exhibited a capacitance of 1 133.3 F/g at a current density of 2 A/g and 688.8 F/g at 20 A/g (5.3 F/cm<sup>2</sup> at 9.4 mA/cm<sup>2</sup> and 3.2 F/cm<sup>2</sup> at 94 mA/cm<sup>2</sup>). In addition, the electrode demonstrated an outstanding cycling stability with the capacitance retention of 90.4% after 3 000 cycles at a current density of 20 A/g. The rational design of LDH based core-

shell architecture may open up new strategies for fabricating promising electrode materials with good energy storage performance for electrochemical energy storage.

## 1 Experiment

### 1.1 Material preparation

All chemicals were of analytical grade and used as received without any further treatment.

Synthesis of 1-D  $\text{Co}_3\text{O}_4$  nanowires on NF: Typically, 1.16 g of  $\text{Co}(\text{NO}_3)_2 \cdot 6\text{H}_2\text{O}$  was dissolved into 50 mL of deionized water to form a homogeneous pink solution, then 1.20 g of urea were added. A piece of NF was pretreated successfully with 6.0 M HCl, deionized water, and absolute ethanol, each for 15 min, to ensure a clean surface. After that, the above prepared aqueous solution and the pretreated NF(10 mm×10 mm×1 mm) were transferred into a 100-mL Teflon-lined stainless-steel autoclave, which was sealed and maintained at 95 °C for 10 h, and then cooled down to ambient temperature naturally. Finally, the product with NF was taken out, washed, vacuum dried and then thermally treated at 250 °C in air for 1 h. The mass of  $\text{Co}_3\text{O}_4$  on NF was determined by subtracting the weight before deposition from the weight after calcination.

Synthesis of  $\text{Co}_3\text{O}_4$ @LDH nanoarrays on NF:  $\text{Co}_3\text{O}_4$ @LDH core-shell structures were prepared by growing NiAl LDH onto  $\text{Co}_3\text{O}_4$  surface via a liquid phase deposition method. 0.11 mol of  $\text{Ni}(\text{NO}_3)_2 \cdot 6\text{H}_2\text{O}$  was dissolved in 200 mL of water with vigorous stirring, and pH was adjusted to 7.5 with a certain amount of aqueous ammonia (28% in volume). The collected precipitate was repeatedly washed with water and dried at ambient temperature and then poured into 40 mL of 0.66 M  $\text{NH}_4\text{F}$  for 48 h under continuous magnetic stirring at ambient temperature. The dispersion was filtered to obtain the Ni parent solution. Typically, the as-synthesized  $\text{Co}_3\text{O}_4$  on NF was immersed in a 100-mL Teflon autoclave with the freshly prepared Ni parent solution, 20 mL of 0.5 M  $\text{H}_3\text{BO}_3$ , 5 mL of 0.05 M  $\text{Al}(\text{NO}_3)_3 \cdot 9\text{H}_2\text{O}$ , and 5 mL of deionized water;

the autoclave was heated in an oven at 120 °C for 10 h. The product with NF substrate was washed with deionized water and ethanol to remove surface ions and molecules by using an ultrasonic bath cleaner, and then dried at 50 °C for 24 h to remove the adsorbed solvents. The mass of NiAl LDH can be determined by subtracting the weight before deposition from the weight after deposition.

## 1.2 Material characterizations

X-ray diffraction (XRD, Bruker D8 Advance X-ray) of the samples was performed using Cu K $\alpha$  radiation ( $\lambda=0.154\ 06\ \text{nm}$ ) at 40 kV and 30 mA. The scanning speed was 5 °/min with a 0.02° step. The morphology and structural properties of the samples were observed by field emission scanning electron microscopy (FESEM, LEO-1550) with an applied voltage of 5 kV and transmission electron microscope (TEM, JEM-2100F).

## 1.3 Electrode preparation and electrochemical measurements

Each electrode was measured in a three-electrode system in 6 M KOH aqueous electrolyte at room temperature with a platinum foil and an Hg/HgO electrode used as the counter and reference electrodes, respectively. Co<sub>3</sub>O<sub>4</sub> and Co<sub>3</sub>O<sub>4</sub>@LDH growing on NF were directly used as working electrodes, respectively. A ZIVE SP2 electrochemical working station instrument was employed for cyclic voltammetry (CV) and galvanostatic charge/discharge (GCD) measurements. CV tests were performed between 0 and 0.65 V (vs Hg/HgO) at different scan rates. GCD curves were measured in the potential range of 0 to 0.6 V (vs Hg/HgO) at different current densities. Cycle stability measurements were tested at 20 A/g for 3 000 cycles.

# 2 Results and Discussion

## 2.1 Synthesis and characterizations

Fig. 1 presents the morphology of the NF substrate, Co<sub>3</sub>O<sub>4</sub> and Co<sub>3</sub>O<sub>4</sub>@LDH on NF. Fig. 1(a) shows the SEM image of the blank NF,

which has smooth surface with a 3-D cross-linked macroporous structure for providing a high surface to facilitate sufficient loading of electroactive species.

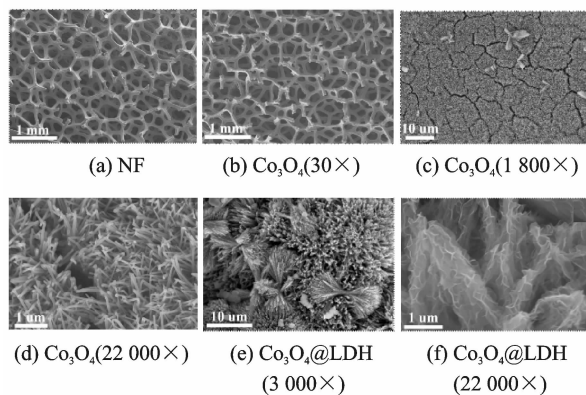


Fig. 1 SEM images of NF, Co<sub>3</sub>O<sub>4</sub> and Co<sub>3</sub>O<sub>4</sub>@LDH

After hydrothermal and heat treatment, it can be observed that the smooth surface of NF is covered by 1-D well-aligned Co<sub>3</sub>O<sub>4</sub> nanowires with an uneven surface texture (Figs. 1(b) and (c)). Besides, a small number of aggregations inlay on the nanowires (Fig. 1(d)). The average diameter of the nanowire is determined to be 50—100 nm and the length can be up to several micrometers. After liquid phase deposition, NiAl LDH covers on the whole surface of Co<sub>3</sub>O<sub>4</sub> nanowires to form a 3-D hierarchical core-shell structure (Fig. 1(e)). The NiAl LDH nanosheets are interconnected with each other, keeping a highly porous configuration (Fig. 1(f)). The pores or voids between the nanosheets and nanowires of both the core and shell are beneficial to the electrolyte infiltration, and the interconnected structures allow fast ion and electron transportation. Intriguingly, the aggregations in-laid on nanowires have become dumbbell shape structure which are composed of porous core-shell nanoarrays.

More detailed structural information was also investigated by TEM. TEM image of a single Co<sub>3</sub>O<sub>4</sub> nanowire in Fig. 2(a) shows that the nanowire with a 70 nm diameter is composed of numerous particles, which is consistent with the SEM result (Fig. 1(d)) and many pores are widely distributed on the surface which result from

the release of  $\text{H}_2\text{O}$  and  $\text{CO}_2$  gas during pyrolysis. Comparatively, the  $\text{Co}_3\text{O}_4 @ \text{LDH}$  in Fig. 2 (b) possess a peculiar core-shell structure in which thin NiAl LDH nanosheets uniformly cover the surface of the porous  $\text{Co}_3\text{O}_4$  nanowire.

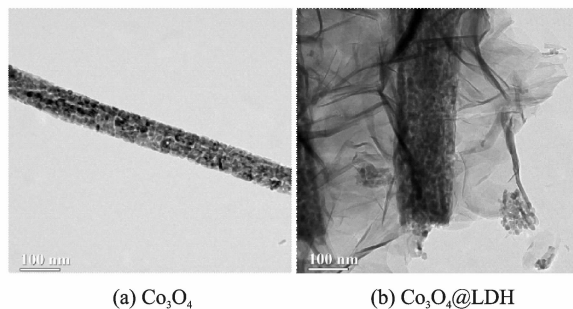


Fig. 2 TEM images of  $\text{Co}_3\text{O}_4$  and  $\text{Co}_3\text{O}_4 @ \text{LDH}$

The phase and structures of  $\text{Co}_3\text{O}_4$  and  $\text{Co}_3\text{O}_4 @ \text{LDH}$  on NF were examined by XRD. As shown in Fig. 3, the three strongly peaks marked by “•” belong to the NF substrate (JCPDS card No: 04-0850). The  $\text{Co}_3\text{O}_4$  nanowires corresponds with the reported pattern of cubic phase  $\text{Co}_3\text{O}_4$  (JCPDS card No: 42-1467). After the second step growth, other diffraction peaks appear in the XRD pattern of the hybrid structure, which can be well index with hydrotalcite-like  $\text{Ni}_6\text{Al}_2(\text{OH})_{16}(\text{CO}_3, \text{OH}) \cdot 4\text{H}_2\text{O}$  (JCPDS card No: 15-0087).

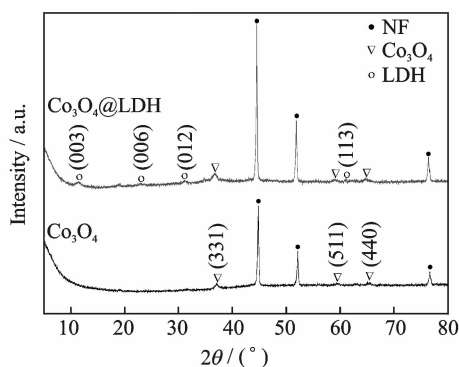
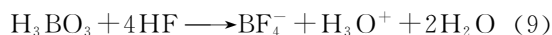
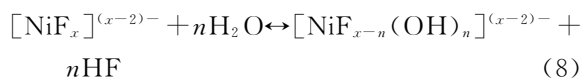
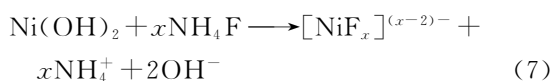
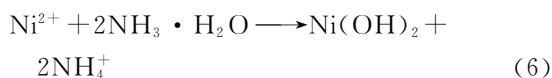
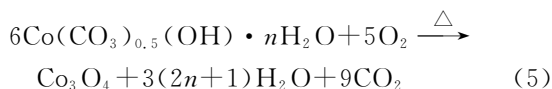
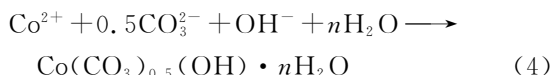
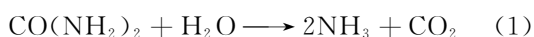


Fig. 3 XRD patterns of  $\text{Co}_3\text{O}_4$  and  $\text{Co}_3\text{O}_4 @ \text{LDH}$

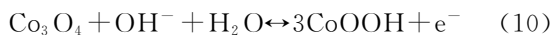
The synthesis approach of 3-D porous  $\text{Co}_3\text{O}_4 @ \text{LDH}$  architecture on the NF involves hydrothermal precipitation, heat treatment and a further liquid phase deposition process. The reactions are illustrated as follows



Initially, a uniform pink precursors  $\text{Co}(\text{CO}_3)_{0.5}(\text{OH}) \cdot n\text{H}_2\text{O}$  were grown directly on NF substrate via a facile hydrothermal reaction of  $\text{Co}^{2+}$  and urea (Reactions 1–4); and further annealing process enabled successive release and loss of  $\text{CO}_2$  and  $\text{H}_2\text{O}$  to form black porous  $\text{Co}_3\text{O}_4$  nanowires (Reaction 5)<sup>[18]</sup>; after that, the obtained porous nanowires were designed as a scaffold for the following structural construction of growing NiAl LDH through a liquid phase deposition method (Reactions 6–9)<sup>[10]</sup>. Finally, the hierarchical  $\text{Co}_3\text{O}_4 @ \text{LDH}$  core-shell structure were prepared and the color of the NF surface turned into deep brown after the formation of NiAl LDH nanosheets onto the  $\text{Co}_3\text{O}_4$  nanowires.

## 2.2 Electrochemical characterizations of electrodes

To investigate the electrochemical properties of  $\text{Co}_3\text{O}_4$  and  $\text{Co}_3\text{O}_4 @ \text{LDH}$ , CV and GCD measurements were conducted. Fig. 4 (a) shows the CV curves of electrodes at a scan rate of 5 mV/s. Redox peaks could be clearly observed for each curve, which is a typical characteristic of faradaic behavior of  $\text{Co}_3\text{O}_4$  and NiAl LDH. For  $\text{Co}_3\text{O}_4$ , the redox peaks are ascribed to the conversion of  $\text{Co}_3\text{O}_4$  to  $\text{CoOOH}$  and  $\text{CoOOH}$  to  $\text{CoO}_2$ , described as follows<sup>[19]</sup>



The peaks of NiAl LDH are attributed to the faradaic redox process of  $\text{Ni}^{2+} / \text{Ni}^{3+}$  based on the following reaction<sup>[20]</sup>



In the case of  $\text{Co}_3\text{O}_4$ @LDH sample, the integral area increases obviously, indicating that this core-shell electrode possesses a significantly

higher specific capacitance and electrochemical activity than individual  $\text{Co}_3\text{O}_4$  electrode. A comparison of the GCD curves at a current density of 2 A/g further demonstrates this (Fig. 4(b)).

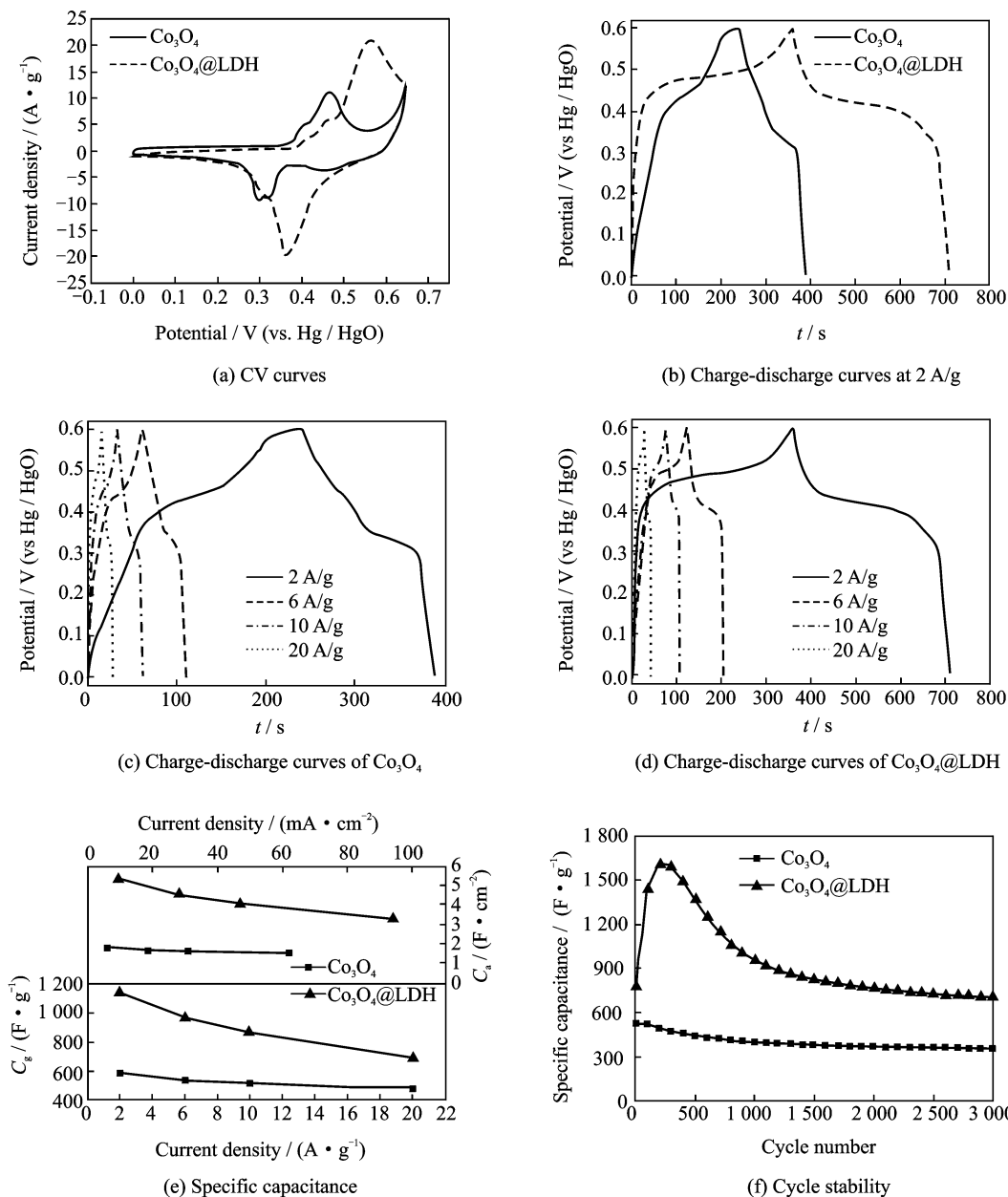


Fig. 4 Electrochemical measurements of  $\text{Co}_3\text{O}_4$  and  $\text{Co}_3\text{O}_4$ @LDH

The charge/discharge characteristics of all these samples exhibit typical faradaic behavior and is consistent with the results of CV curves. Areal ( $C_a$ ) and gravimetric capacitance ( $C_g$ ) can be calculated from the GCD curves, respectively (Eqs. (13) and (14))

$$C_a = I \times \Delta t / (S \times \Delta V) \quad (13)$$

$$C_g = I \times \Delta t / (m \times \Delta V) \quad (14)$$

where  $I$  is the discharge current (A),  $\Delta t$  the discharge time (s),  $S$  the geometrical area of the electrode,  $\Delta V$  the potential range (V), and  $m$  the mass of the electroactive material in the electrode (g). The corresponding  $C_g$  of  $\text{Co}_3\text{O}_4$ @LDH at 2 A/g is measured to be 1 133.3 F/g ( $C_a$ : 5.33

$\text{F}/\text{cm}^2$ ), which is much larger than that of  $\text{Co}_3\text{O}_4$  ( $C_g$ : 583.3  $\text{F}/\text{g}$ ,  $C_a$ : 1.81  $\text{F}/\text{cm}^2$ ). This result reveals the advantage of 3-D core-shell material array for capacitance improvement. The GCD curves of  $\text{Co}_3\text{O}_4$  and  $\text{Co}_3\text{O}_4@\text{LDH}$  electrode tested at various current densities of 2–20  $\text{A}/\text{g}$  were exhibited in Figs. 4(c, d). Each curve has good symmetry, implying excellent electrochemical reversibility and charge-discharge properties. The specific capacitance of  $\text{Co}_3\text{O}_4$  and  $\text{Co}_3\text{O}_4@\text{LDH}$  electrodes derived from the discharging curves at different current densities is compared, as shown in Fig. 4(e). Within the current density from 2 to 20  $\text{A}/\text{g}$ , the 3-D core-shell nanoarrays always delivers a greater  $C_g$  than  $\text{Co}_3\text{O}_4$  (the lower part). At a higher current density of 20  $\text{A}/\text{g}$ , the  $C_g$  of  $\text{Co}_3\text{O}_4@\text{LDH}$  electrode (688.8  $\text{F}/\text{g}$ ) remains at up to 60.8% of that measured at 2  $\text{A}/\text{g}$ , thereby exhibiting good rate capability. The  $C_a$  of two electrodes versus current density plots are also shown in Fig. 4(e) (the upper part). In general, hybrid core-shell nanoarrays still demonstrate apparently superior  $C_a$  compared with the  $\text{Co}_3\text{O}_4$ . At the lowest current density of 9.4  $\text{mA}/\text{cm}^2$ , a capacity of 5.33  $\text{F}/\text{cm}^2$  can be achieved. Moreover, at a higher current density (94  $\text{mA}/\text{cm}^2$ ), the  $C_a$  of the hybrid nanowire array is maintained at 3.24  $\text{F}/\text{cm}^2$ ; strikingly, this value is still much larger than that of  $\text{Co}_3\text{O}_4$  (1.81  $\text{C}/\text{cm}^2$  at the lowest current density of 6.2  $\text{mA}/\text{cm}^2$ ). The above features further demonstrate that the rational incorporation of active materials into well-defined nanostructures can bring a strong synergetic effect on the final capacitive properties.

The electrochemical stability of  $\text{Co}_3\text{O}_4$  and  $\text{Co}_3\text{O}_4@\text{LDH}$  electrodes were tested for 3 000 charge-discharge cycles at a current density of 20  $\text{A}/\text{g}$ , as shown in Fig. 4(f). For both electrodes, an increase in specific capacitance during the initial cycles is observed, which could result from the activation process of  $\text{Co}_3\text{O}_4$  or NiAl LDH. Thereafter, two electrodes suffer from a loss of specific capacitance during the subsequent

cycles. For the  $\text{Co}_3\text{O}_4$  electrode, a  $C_g$  value of 347.6  $\text{F}/\text{g}$  (decreases by 33.6% of its initial capacitance) can be maintained after 3 000 cycles. In the case of  $\text{Co}_3\text{O}_4@\text{LDH}$  electrode, the specific capacitance keeps at about 705.7  $\text{F}/\text{g}$  after 3 000-cycle test with a retention rate of 90.4%, showing the excellent cycling stability. This observation is attributed to the structural instability of NiAl LDH materials during the cycling test, which was confirmed from the SEM images (Fig. 5) of the  $\text{Co}_3\text{O}_4$  and  $\text{Co}_3\text{O}_4@\text{LDH}$  electrodes after the cycle tests at 20  $\text{A}/\text{g}$ . It can be observed that the  $\text{Co}_3\text{O}_4$  nanowires exhibit small bending deformation (Fig. 5(a)) compared with the initial morphology (Figs. 1(c, d)). The nanowires tend to cluster at their tips to form sheaf-like structure, which may be due to the strong interaction forces between the long and thin nanowires. For  $\text{Co}_3\text{O}_4@\text{LDH}$  electrode (Fig. 5(b)), it maintains the original 3-D core-shell structure except that some of the interconnected nanosheets decrease. No cluster based sheaf-like structure can be observed compared with  $\text{Co}_3\text{O}_4$  electrode due to the existence of interconnected NiAl LDH nanosheets. The reported results imply that the combination of  $\text{Co}_3\text{O}_4$  and NiAl LDH with a unique core-shell morphology and independent electroactivities into a single engineered hybrid architecture can substantially enhance the electrochemical properties. It is believed that the synergistic contribution from 1-D porous  $\text{Co}_3\text{O}_4$  nanowires, ultrathin NiAl-LDH nanosheets, and the ordered array configuration should account for the good electrochemical performance.

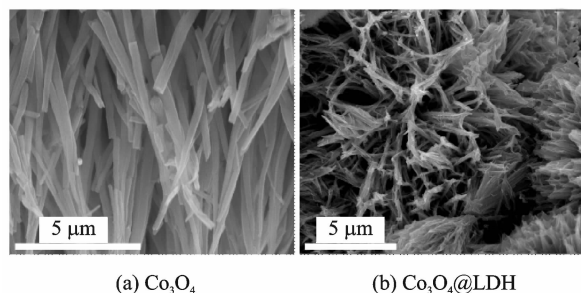


Fig. 5 SEM images of  $\text{Co}_3\text{O}_4$  and  $\text{Co}_3\text{O}_4@\text{LDH}$  electrodes after cycling test at 20  $\text{A}/\text{g}$

Our results demonstrate the importance and great potential application of 3-D self-supported  $\text{Co}_3\text{O}_4$ @LDH core-shell materials in the development of high performance energy storage systems. The excellent supercapacitive property of 3-D porous  $\text{Co}_3\text{O}_4$ @LDH electrode could be attributed to the following reasons: (1) The core-shell architecture is composed of  $\text{Co}_3\text{O}_4$  core and NiAl LDH shell in which a synergistic effect will play a role; (2) 1-D  $\text{Co}_3\text{O}_4$  nanowires grown directly on NF improves conductivity, offering effectively electron transport to NiAl LDH nanosheets; (3) NiAl LDH nanosheets are strongly anchored on the  $\text{Co}_3\text{O}_4$  nanowires to form the unique hierarchical core-shell structure with good stability and integrity; (4) the pores and voids are favorable to electrolyte infiltration and the rapid diffusion of ions by providing low-resistance pathways through the electrode surface.

### 3 Conclusions

Three-D porous  $\text{Co}_3\text{O}_4$ @LDH core-shell electrode grown directly on nickel foam has been successfully synthesized through hydrothermal precipitation, heat treatment and a further liquid phase deposition process. The obtained porous electrode shows outstanding electrochemical performance, which can be attributed to the synergistic contribution from the two promising materials ( $\text{Co}_3\text{O}_4$  and NiAl LDH), together with the merits of 3-D core-shell nanoarray architecture. We believe that the work presented here not only suggests the possibility to engineer  $\text{Co}_3\text{O}_4$  and NiAl LDH into promising electrode materials, but presents a new way to create hybrid electrode architectures for energy storage devices, wearable and portable electronics.

### Acknowledgements

This work was supported by the Basic Science Research Program through the National Research Foundation of Korea funded by the Ministry of Education, Science and Technology (No. 2014R1A1A2055740) and the Start-up Research Grant (No. SRG2015-00057-FST).

### References:

- [1] SIMON P, GOGOTSI Y, DUNN B. Where do batteries end and supercapacitors begin? [J]. *Science*, 2014, 343(6176):1210-1211.
- [2] LIU L B, YU Y, YAN C, et al. Wearable energy-dense and power-dense supercapacitor yarns enabled by scalable graphene-metallic textile composite electrodes [J]. *Nature Communications*, 2015, 6: 7260.
- [3] SHEN L F, CHE Q, LI H S, et al. Mesoporous  $\text{NiCo}_2\text{O}_4$  nanowire arrays grown on carbon textiles as binder-free flexible electrodes for energy storage[J]. *Advanced Functional Materials*, 2014, 24(18):2630-2637.
- [4] WAND J, DING B, XU Y L, et al. Crumpled nitrogen-doped graphene for supercapacitors with high gravimetric and volumetric performances [J]. *ACS Applied Materials & Interfaces*, 2015, 7(40):22284-22291.
- [5] DINH T M, ACHOUR A, VIZIREANU S, et al. Hydrus  $\text{RuO}_2$ /carbon nanowalls hierarchical structures for all-solid-state ultrahigh-energy-density micro-supercapacitors[J]. *Nano Energy*, 2014, 10:288-294.
- [6] YU N, YIN H, ZHANG W, et al. High-performance fiber-shaped all-solid-state asymmetric supercapacitors based on ultrathin  $\text{MnO}_2$  nanosheet/carbon fiber cathodes for wearable electronics[J]. *Advanced Energy Materials*, 2016, 6(2):1501458-1501466.
- [7] GOPALAKRISHNAN K, SULTAN S, GOVINDARAJ A, et al. Supercapacitors based on composites of PANI with nanosheets of nitrogen-doped RGO, BC1.5N,  $\text{MoS}_2$  and  $\text{WS}_2$  [J]. *Nano Energy*, 2015, 12:52-58.
- [8] ZHU Y, MURALI S, STOLLER M D, et al. Carbon-based supercapacitors produced by activation of graphene[J]. *Science*, 2011, 332(6037):1537-1541.
- [9] WANG J, DING B, HAO X D, et al. A modified molten-salt method to prepare graphene electrode with high capacitance and low self-discharge rate[J]. *Carbon*, 2016, 102:255-261.
- [10] ZHANG L J, WANG J, ZHU J J, et al. 3D porous layered double hydroxides grown on graphene as advanced electrochemical pseudocapacitor materials[J]. *Journal of Materials Chemistry A*, 2013, 1(32):9046-9053.
- [11] ZHANG L, HUI K N, HUI K S, et al. High-performance hybrid supercapacitor with 3D hierarchical porous flower-like layered double hydroxide grown on nickel foam as binder-free electrode [J]. *Journal of*

- Power Sources, 2016,318:76-85.
- [12] YU C, YANG J, ZHAO C T, et al. Nanohybrids from NiCoAl-LDH coupled with carbon for pseudocapacitors: Understanding the role of nano-structured carbon[J]. *Nanoscale*, 2014,6(6):3097-3104.
- [13] YANG J, YU C, FAN X, et al. 3D architecture materials made of NiCoAl-LDH nanoplates coupled with NiCo-carbonate hydroxide nanowires grown on flexible graphite paper for asymmetric supercapacitors [J]. *Advanced Energy Materials*, 2014,4(18):1400761-1400768.
- [14] XIONG X, DING D, CHEN D, et al. Three-dimensional ultrathin Ni(OH)<sub>2</sub> nanosheets grown on nickel foam for high-performance supercapacitors[J]. *Nano Energy*, 2015,11:154-161.
- [15] ZHANG F, YUAN C, LU X, et al. Facile growth of mesoporous Co<sub>3</sub>O<sub>4</sub> nanowire arrays on Ni foam for high performance electrochemical capacitors [J]. *Journal of Power Sources*, 2012,203:250-256.
- [16] LU Z, YANG Q, ZHU W, et al. Hierarchical Co<sub>3</sub>O<sub>4</sub>@Ni-Co-O supercapacitor electrodes with ultrahigh specific capacitance per area[J]. *Nano Research*, 2012, 5(5):369-378.
- [17] WANG J, ZHANG X, WEI Q, et al. 3D self-supported nanopine forest-like Co<sub>3</sub>O<sub>4</sub>@CoMoO<sub>4</sub> core-shell architectures for high-energy solid state supercapacitors[J]. *Nano Energy*, 2016, 19:222-233.
- [18] KONG D Z, LUO J S, WANG Y L, et al. Three-dimensional Co<sub>3</sub>O<sub>4</sub>@MnO<sub>2</sub> hierarchical nanoneedle arrays: Morphology control and electrochemical energy storage[J]. *Advanced Functional Materials*, 2014, 24(24):3815-3826.
- [19] YUAN C Z, YANG L, HOU L R, et al. Growth of ultrathin mesoporous Co<sub>3</sub>O<sub>4</sub> nanosheet arrays on Ni foam for high-performance electrochemical capacitors [J]. *Energy & Environmental Science*, 2012, 5(7):7883-7887.
- [20] LIU X X, WANG C, DOU Y B, et al. A NiAl layered double hydroxide@carbon nanoparticles hybrid electrode for high-performance asymmetric supercapacitors [J]. *Journal of Materials Chemistry A*, 2014, 2(6):1682-1685.

Dr. **Zhang Luojiang** received the B. S. and M. S. degrees in applied chemistry from Nanjing University of Aeronautics and Astronautics (NUAA) in 2009 and 2012, respectively. After receiving the Ph. D. degree from Hanyang University (South Korea), he worked as a postdoctoral researcher in the Department of Chemistry of Pohang University of Science and Technology (POSTECH, Korea) until August 2017. From then, he has been working as a postdoctoral researcher in The Hong Kong Polytechnic University. His research interests and activities cover the synthesis, design and application of novel electrode materials for supercapacitors.

Dr. **Hui Kwan San** received Ph. D. degree in mechanical engineering of Hong Kong University of Science and Technology in 2008. He was a lecturer in Systems Engineering and Engineering Management of City University of Hong Kong (August 2008 to February 2013). In March 2013, he was an assistant professor in Mechanical Convergence Engineering at Hanyang University, Seoul, South Korea. In 2016, he was appointed as a lecturer in Mechanical Engineering of University of East Anglia, UK. He has extensive research experiences in material science, catalysis, air/water pollution control, and energy storage.

(Production Editor: Xu Chengting)